

Comparative performance of between-population allocation strategies for SARS-CoV-2 vaccines

Keya Joshi^{1,*a}, Eva Rumpler^{1,*a}, Lee Kennedy-Shaffer^{a,b}, Rafia Bosan^a and Marc Lipsitch^a

^aCenter for Communicable Disease Dynamics, Department of Epidemiology, Harvard TH Chan School of Public Health, 02115 Boston, Massachusetts

^bDepartment of Mathematics & Statistics, Vassar College, 12604 Poughkeepsie, New York

¹Contributed equally to this work.

*Corresponding authors.

1 Keywords

COVID-19, SARS-CoV-2, vaccine, allocation, distribution

2 Abstract

Vaccine allocation decisions during the ongoing COVID-19 pandemic have proven to be challenging due to competing ethical, practical, and political considerations. Complicating decision making, policy makers need to consider vaccine allocation strategies that balance needs both within and between populations. Due to limited vaccine stockpiles, vaccine doses should be allocated in locations where their impact will be maximized. Using a susceptible-exposed-infectious-recovered (SEIR) model we examine optimal SARS-CoV-2 vaccine allocation decisions across two populations considering the impact of population size, underlying immunity, continuous vaccine roll-out, and heterogeneous population risk structure. We find that in the context of an emerging pathogen, where many epidemiologic characteristics might not be known, equal vaccine allocation between populations performs optimally in most scenarios. In the specific case considering heterogeneous population risk structure, first targeting individuals at higher risk of transmission or death due to infection leads to equitable resource allocation across populations.

3 Introduction

Since its emergence, SARS-CoV-2 has caused considerable suffering and disruption of societies, resulting in over 173 million infections and 3.7 million deaths worldwide as of June 2021 [1]. Vaccines are currently the most effective public health intervention available against SARS-CoV-2, with eight vaccines currently approved for full use and an additional seven authorized for early or limited use globally [2, 3].

Even with the approval of multiple vaccines, distributed across different regions globally, roll-out has been slow. While some countries are falling far behind their anticipated timelines, vaccination rates are highly unequal across countries [4]. Indeed, as some countries have already vaccinated over 60% of their population, and are on track to vaccinate all willing adults by the end of the summer of 2021, others still do not have access to vaccines [4]. Even as COVAX – a Coalition for Epidemic Preparedness Innovations (CEPI), Gavi the Vaccine Alliance (GAVI) and World Health Organization (WHO) collaboration – aims to deliver approximately 1.8 billion doses to 92 low- and middle-income economies by the end of 2021 [5], it could take up to 2023 [6, 7] for all countries to have access to a sufficient number of doses. Overall, vaccination allocation decisions are currently being made under the constraint of a limited vaccine stockpile and multiple factors need to be considered in order to maximize the effect of each dose across populations.

As previous work [8, 9, 10] has shown, targeting specific subgroups within a given population, including older individuals, results in decreased COVID-19 morbidity and mortality. Further, previous theoretical work [11] has shown that unequal vaccine allocations might be favorable, but are less optimal when incorporating realistic assumptions about population heterogeneity and contact structure. This leaves a potentially conflicting message for policy makers when considering optimal allocation decisions. We build upon this work, by not only considering the optimal decision, but also how the decision compares to all possible allocations across two populations. Our results show that the efficiency gains for unequal allocations that are found in models with highly-simplified epidemics are typically small; moreover, they vanish and can even reverse under settings more relevant to the current pandemic. Similar to previous findings, we show in more realistic scenarios, incorporating population heterogeneity and interaction between populations, equitable distributions are not only optimal, but vastly outperform unequal distributions.

4 Methods

We use a deterministic, two-population, susceptible-exposed-infectious-recovered (SEIR) compartmental model. We assume people are initially susceptible (S). Susceptible individuals move to the exposed state (E) after an effective contact with an infectious individual. After a latent period, exposed individuals become infectious (I). After the infectious period has elapsed, infectious individuals move to a recovered state (R). We do not account for waning immunity and assume once individuals have recovered, they stay immune to SARS-CoV-2 for the duration of our simulation, here modeled as one year, which is longer than the epidemic duration in the vast majority of simulations. We start by assuming that there is no interaction between the two populations, so all disease transitions happen in parallel between the two populations.

We extend the traditional SEIR model to allow for underlying immunity and vaccination (Figure S3). At the start of the epidemic, in each population, individuals can be in the susceptible (S),

45 infectious (I), or recovered (R) compartments. When there is underlying immunity, a set proportion
46 of individuals are placed in R. Individuals in R, whether through underlying immunity or infection
47 through the course of the simulation, can never be re-infected. When vaccine doses are distributed
48 to the population, vaccinated individuals are placed in R if the vaccination is successful. We assume
49 that the vaccine is all-or-nothing with 90% efficacy, meaning 90% of those who are vaccinated are
50 placed in R and the remainder stay in S. When there is underlying immunity and vaccination,
51 immune individuals may be vaccinated; vaccination has no effect on them and they remain in R.
52 Finally, we initialize each simulation by placing one individual in I and allow the epidemic to run,
53 unmitigated except by vaccination, through each population. Full model parameters and equations
54 are shown in SI Appendix A.2.

55
56 To recreate the results of Keeling and Shattock (2012) [11], we model two homogeneous populations
57 with identical characteristics apart from population size. In this scenario we assume population
58 2 is double the size of population 1 (Figure 2). For later scenarios, which consider the impact of
59 heterogeneity within populations, we simulate two populations that are identical in size, but vary
60 in their population characteristics (e.g. fraction high risk) (Figure 5 and 6).

61
62 Next, we extend the model by allowing for heterogeneous risk groups. Within each population,
63 we first model efficient transmitters of the SARS-CoV-2 virus (e.g. young adults) [12]. In this
64 scenario, we assume high-transmitters are four times more likely to transmit compared to other
65 groups. We fix the within-population structure to allow the global R_0 to equal 2. The full deriva-
66 tion is shown in SI Appendix A.2.4.

67
68 In addition, we also model individuals at elevated risk of death from severe COVID-19 disease,
69 which can represent elderly individuals or other individuals with co-morbidities known to exacer-
70 bate COVID-19 disease [13, 14]. For simplicity of the model, we assume these individuals are five
71 times more likely to die than other individuals infected with SARS-CoV-2. Note that death rates
72 are assumed to be constant throughout the epidemic, which may not be realistic as health care
73 resources are strained by large case loads or case management improves over time.

74
75 Similarly to the homogeneous two population scenario described above, we initialize the model
76 by placing individuals from each population in the susceptible or recovered state based on the
77 pre-existing immunity level and the vaccine allocation scenario. The total number of vaccine doses
78 are split amongst the two populations based on the scenario. Within each population, high-risk
79 individuals are vaccinated first, with leftover doses then allocated to the low-risk population, as
80 described in SI Appendix A.2.5.

81
82 Finally, we model the scenario where vaccines are unavailable at the start of the epidemic, but
83 are slowly rolled out over the course of the epidemic. For this simulation we vary both the timing
84 of roll-out, and the fraction of the population vaccinated each day. We allow vaccine roll-out to start
85 1, 10, 30, 50, or 100 days after the epidemic has begun and vary the proportion of the population
86 vaccinated from 1% to 3% per day. For these simulations, the vaccine is allocated within and across
87 populations identically to the scenarios described above for the homogeneous and heterogeneous
88 scenarios.

89
90 For each simulation we calculate the cumulative number of infections and deaths from the determin-
91 istic SEIR model at the end of the epidemic. Across each scenario we define the optimal allocation
92 strategy as the one that minimizes the total epidemic size (cumulative number of infections) across

93 both populations. Within the high morbidity scenario, we define the optimal allocation strategy as
94 the one that minimizes the total number of deaths across both populations. This is equivalent to
95 maximizing the total number of people across both populations that escape infection (or death) [15].

96
97 We conduct sensitivity analyses to assess the robustness of our results. First, we model a leaky
98 vaccine scenario where we assume the vaccine reduces susceptibility to SARS-CoV-2 by 90%. As a
99 result, all vaccinated individuals (except those previously immune through natural infection) can
100 become infected with the virus, although the probability of infection for each contact with an in-
101 fected individual is lower than for an unvaccinated individual. We further extend the model by
102 relaxing the assumption that the two populations do not interact. We allow a fraction i of infected
103 individuals in both populations to contribute to the force of infection in the other population in-
104 stead of their own population. An i value of 0 corresponds to no interaction, and an i value of 0.5
105 corresponds to complete interaction between the two populations (i.e. is equivalent to one large
106 population). Full model equations are shown in SI Appendix A.2.3.

107
108 All analyses were conducted in R version 4.0.3.

109 **5 Results**

110 **5.1 Literature review**

111 We reviewed the literature on optimal vaccine allocation across populations that was published
112 prior to the emergence of SARS-CoV-2 (see SI Table A.3.1). Multiple papers [11, 16, 17, 18, 19]
113 have shown that allocation proportional to population size is rarely optimal. Further, previous
114 studies have highlighted that the timing of vaccine allocation [20, 21, 22], heterogeneity in popula-
115 tion composition, as well as the stochasticity in infection dynamics affect the optimal distribution
116 [23, 24]. Duijzer et al. (2018) [15] provide important contributions by showing that the optimal
117 vaccination threshold is often not the herd immunity threshold.

118
119 Additionally, we summarize some of the recent literature modeling optimal SARS-CoV-2 vaccine
120 allocation in one population in SI Table A.3.2.

121 **5.2 Optimal allocation in two populations of equal size**

122 We build upon the existing literature by first examining allocation decisions in the simple scenario
123 of two identical, non-interacting populations with no underlying SARS-CoV-2 immunity (see Figure
124 1). In the simplest case, with a small number of vaccine doses available, pro-rata allocation performs
125 comparably to highly unequal allocation strategies. As the number of vaccine doses increases, highly
126 unequal strategies gain advantage over pro-rata allocation. This occurs because one population can
127 be vaccinated close to, but lower than, its herd immunity threshold, maximizing the indirect effect
128 of the vaccine doses [15]. When sufficient vaccines are available for both populations to reach that
129 threshold, more unequal strategies use the doses less efficiently, as indicated by the increasing arms
130 of the “W” shapes in Figure 1. Allocating doses to the population that has reached its threshold
131 provides limited benefit in that population and withholds doses from the other. When there are
132 nearly enough doses to reach the thresholds in both populations, the optimal strategy becomes
133 equal allocation between the two populations.

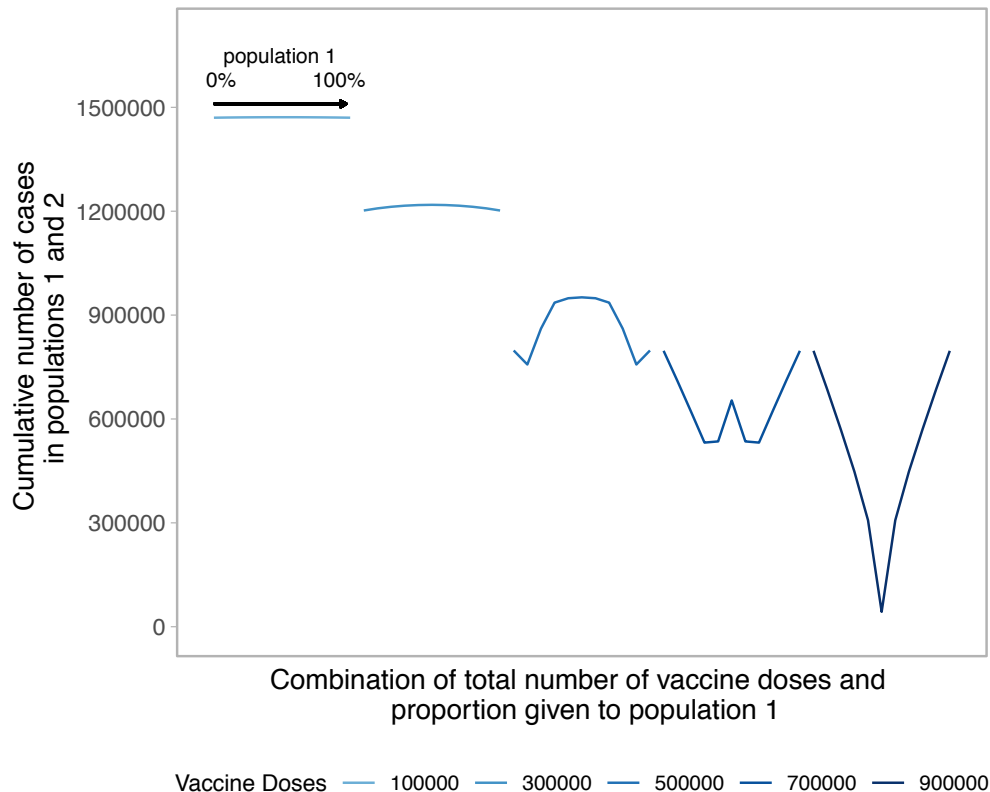


Figure 1: Performance of different allocation strategies of a limited SARS-CoV-2 vaccine stockpile across two homogeneous population of equal size with no underlying immunity and prophylactic vaccination. Both populations have one million individuals. Each color represents a different number of total vaccine doses. Each curve shows the cumulative number of COVID-19 cases across both population 1 and 2 for different proportions of doses given each population. Across each curve, the proportion of doses to population 1 goes from 0 to 100%.

134 5.3 Optimal allocation in two populations of unequal size

135 Extending the simple case of non-interacting populations of equal size, previous studies have shown
 136 how optimal allocation across populations of different sizes is not linear, but varies with the number
 137 of doses available in a characteristic, and often counter-intuitive, “switching” pattern [11, 15, 17].

138
 139 As shown in Figure 2 (top), when the number of doses available is very limited, optimal allo-
 140 cation concentrates all vaccine doses to the smallest population, not assigning any to the largest
 141 population (regime 1). As the number of doses allocated to the smaller population reaches its
 142 threshold, additional doses are gradually allocated to the larger population (regime 2). Strikingly,
 143 for 777,500 doses available, a drastic switch happens and all doses are allocated to the larger pop-
 144 ulation and none to the smaller one (regime 3). Then, as the largest population itself reaches
 145 its threshold, supplementary doses are assigned to the smaller population (regime 4). When the
 146 number of vaccines available allows both populations to attain their respective thresholds, vaccines
 147 are allocated proportionally to the population sizes (regime 5).

148
 149 For most values of vaccine available, the optimal allocation is highly unequal, as previously shown

150 [11, 15]. This counterintuitive result is caused by the non-linearity of the indirect effect from each
151 additional vaccine dose. Additional doses are allocated to the population where they have the
152 largest benefit. For example, in regime 1 of Figure 2, additional doses bring a larger benefit in the
153 smaller population than they would in the larger population.

154

155 Importantly, while prior literature [11] demonstrates that unequal allocations can be optimal, these
156 results show that the benefit of such unequal, optimal allocations over more nearly equal ones is
157 often small. As shown in Figure 2 (bottom), for low numbers of vaccine doses (regimes 1 and
158 2), although concentrating all doses to the smallest population is optimal, other strategies do not
159 perform much worse. Each regime is characterized by a different allocation profile that gives rise
160 to a different optimum, indicated by black points. In regime 4, the characteristic W shape appears
161 where a fully unequal allocation is sub-optimal, regardless of which population is vaccinated.

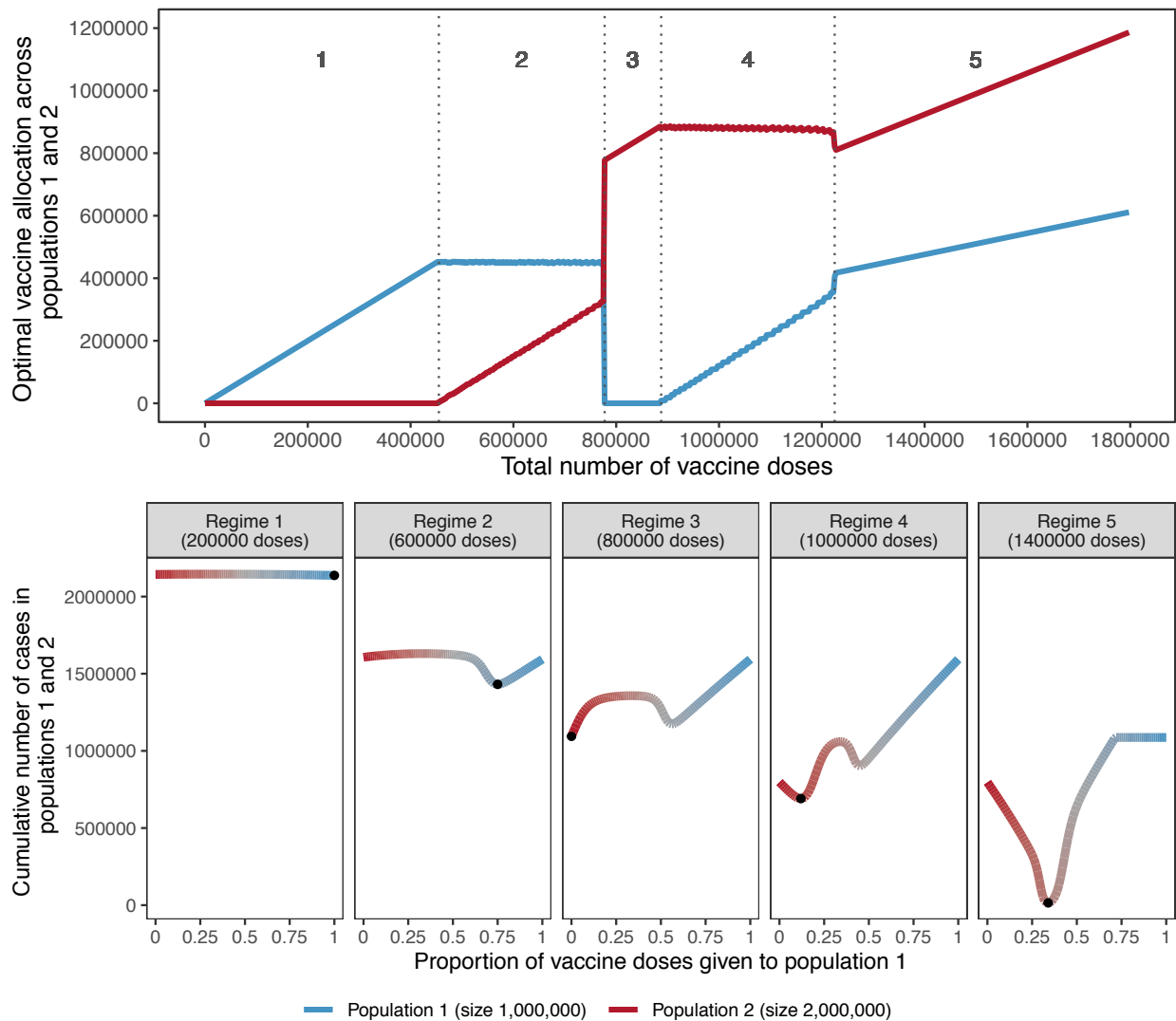


Figure 2: Top: Optimal allocation strategies of a limited SARS-CoV-2 vaccine stockpile across two homogeneous populations of unequal size with no underlying immunity and prophylactic vaccination. Populations 1 (blue) and 2 (red) have one and two million individuals, respectively. Dashed vertical lines were added to highlight regimes (1 to 5) showing different vaccine allocation patterns. Bottom : Performance of allocation strategies for five different numbers of vaccine doses, representative of the regimes shown in the top half of the Figure. Color coding corresponds to vaccine allocation ranging from giving all doses to population 2 (red) to giving all doses to population 1 (blue). The optimal allocation, the minimal value on each plot, is highlighted by a black point.

162 5.4 Impact of underlying immunity

163 As vaccines continue to get rolled out at varying speeds, populations will have varying degrees of
 164 underlying immunity to the virus due to prior infections. Serological surveys estimate that around
 165 a fifth of the population had already been infected in areas hardest hit during the spring of 2020
 166 (23% in NYC [25], 18% in London [26] and 11% in Madrid and Paris [27, 28]). Select high-risk
 167 groups, including health care workers and nursing home residents, have been shown to have an
 168 even higher prevalence of SARS-CoV-2 antibodies [29]. To account for underlying immunity, we

169 further simulate optimal allocation decisions with varying levels of underlying immunity in each
 170 population to mirror the fact that allocation decisions are made during an ongoing pandemic.

171

172 Comparing two populations with varying amounts of underlying immunity, the optimal strategy
 173 favors prioritizing the population that is closer to their herd immunity threshold (Figure 3). Figure
 174 3 shows optimal allocation decisions across two homogeneous populations of equal size with no
 175 immunity (top left, repeating Figure 1) or increasing degrees of immunity in population 1. With
 176 increasing immunity in population 1, the characteristic V- or W-shape becomes more lopsided as
 177 fewer doses are required in population 1 to reach the threshold at which doses should be split be-
 178 tween populations. Extremely unequal allocation strategies either waste doses or fail to minimize
 179 the cumulative number of infections in both populations if given completely to population 1 or 2,
 180 respectively. In addition, allocating vaccines to population 1 beyond the amount needed to reach
 181 its threshold results in the highest cumulative number of COVID-19 cases because it confers little
 182 additional benefit in population 1, and deprives population 2 of vaccines needed to mitigate cases.
 183 As before, once the number of doses is large enough to approach or reach the threshold in both
 184 populations, optimal strategies move to a more equitable approach.

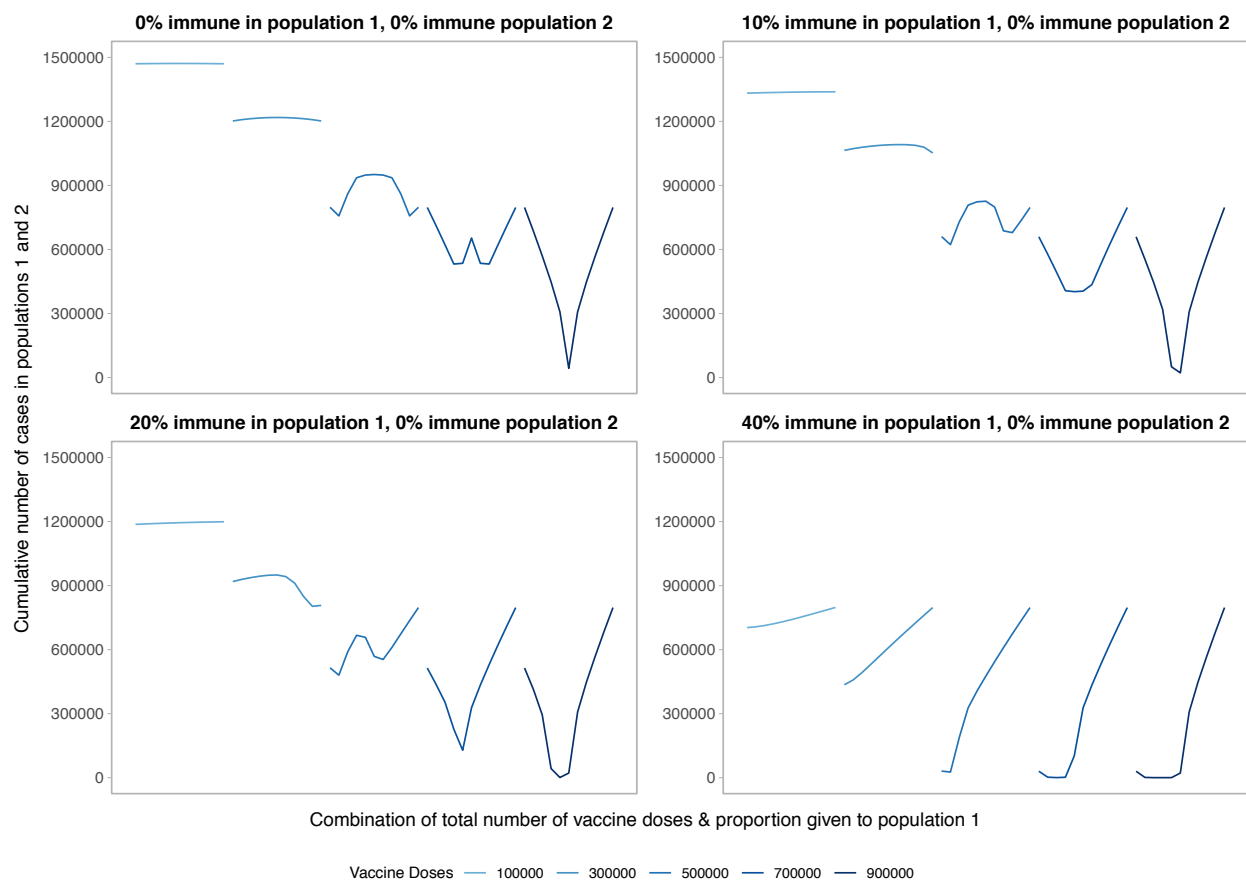


Figure 3: Performance of different allocation strategies of a limited SARS-CoV-2 vaccine stockpile across two homogeneous populations of equal size (one million individuals) with different underlying immunity, and prophylactic vaccination. We fix population 2 to have no underlying SARS-CoV-2 immunity and vary underlying immunity in population 1 from 0 to 40%. The panel on the top left is equivalent to Figure 1.

185 5.5 Impact of delayed vaccine roll-out in a homogeneous population

186 Next, we examine the impact of vaccine roll-out over the course of the epidemic. We find both the
187 timing and speed of roll-out play an important role in minimizing the final size of the epidemic.
188 As shown in Figure 4, the cumulative number of cases across both populations is minimized when
189 vaccine roll-out occurs as soon as possible after the start of the epidemic. Further, the final size is
190 minimized when roll-out speed is increased, vaccinating a larger proportion of the population each
191 day.

192

193 For the early and efficient roll-out (10 days and speed of 2 or 3% of the population/day), the
194 vaccination performance profile looks similar to that of prophylactic vaccine deployment strategy
195 shown in Figure 1. However for slower or later roll-out we see highly unequal approaches per-
196 form poorly across almost all doses and more equitable approaches result in the smallest final size.
197 This is because a larger fraction of the population is naturally infected, minimizing the gains from
198 concentrating vaccine doses in one population.

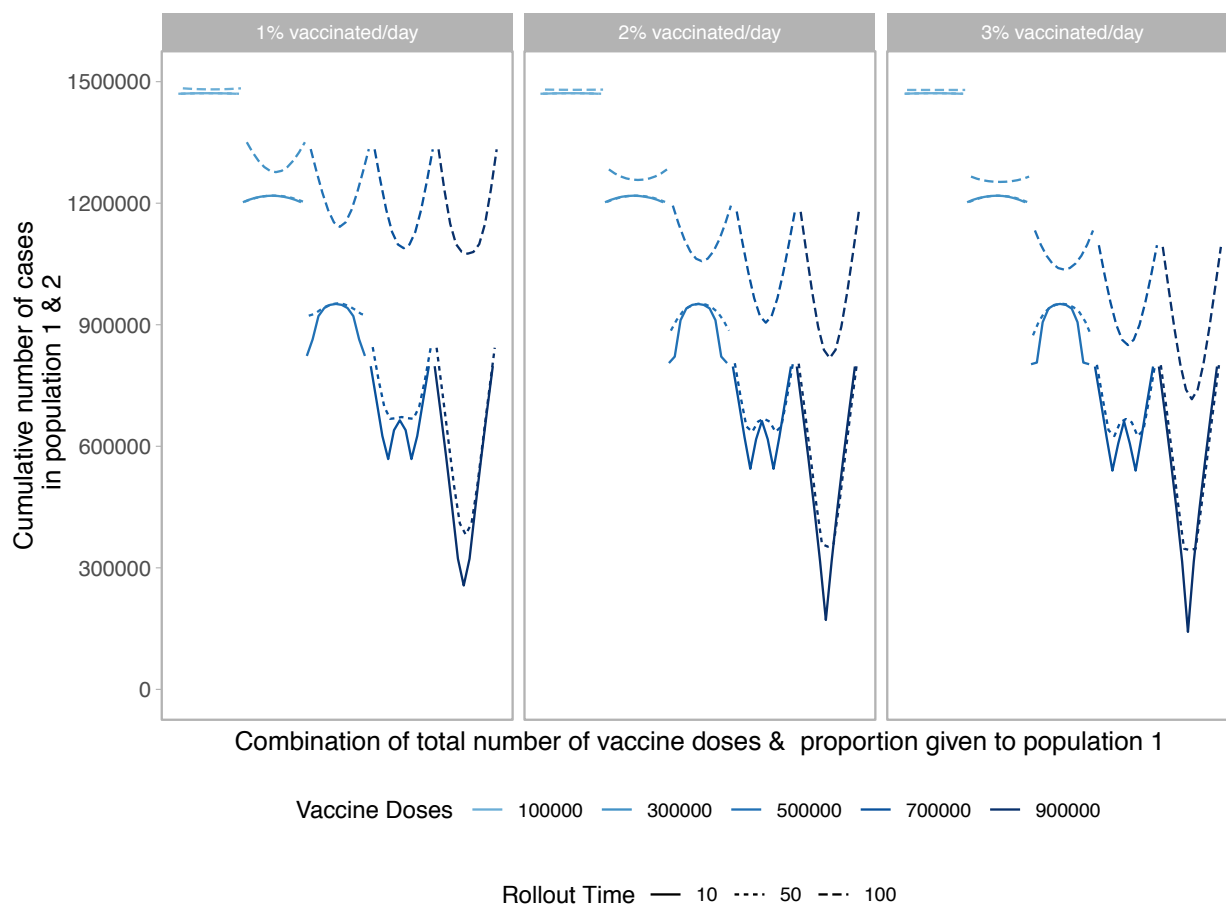


Figure 4: Performance of different allocation strategies of a limited SARS-CoV-2 vaccine stockpile across two homogeneous populations of equal size (one million individuals) with no underlying immunity, with vaccines rolled out at different speeds and different times after the start of the epidemic. We vary both the timing and speed of roll-out between 10, 50 or 100 days after the start of the epidemic with 1, 2, or 3% of the population vaccinated per day.

199 5.6 Impact of heterogeneous population structure

200 Looking within a population, many studies have shown optimal strategies favor prioritizing older
201 individuals (e.g., those aged 60 or over) when the goal is minimizing mortality. If the goal instead
202 is minimizing final size, targeting adults 20-49 with an effective transmission-blocking vaccine mini-
203 mizes cumulative incidence [8, 9]. Here we model the impact of heterogeneous population structure
204 to examine the impact of strategies across populations. These simulations consider populations
205 with heterogeneous transmission or with heterogeneous risk of death.

206

207 Targeting high transmission or high mortality groups first within a population shifts the opti-
208 mal allocation across the two populations in the direction of greater equity (Figure 5 and 6). In
209 Figure 5 we first model the impact of prophylactic vaccination in a heterogeneous population struc-
210 ture with 25% of each population at either high risk of transmission (top) or death (bottom). In
211 the high-transmission scenario, the behavior looks similar to that in Figure 1 for a low number
212 of doses, representing the trade-off between vaccinating the high-transmitters in both populations.
213 Once there are enough doses available to vaccinate enough high-transmitters to reduce transmission
214 dramatically, the optimal strategy favors more equitable allocations across the two populations as
215 high-transmitters are driving the bulk of transmission. This shift to more equitable allocations
216 occurs at a lower number of vaccine doses compared to Figure 1. In the high-mortality scenario,
217 we see the optimal allocation rapidly shift to equitable strategies, starting at a very low number of
218 vaccine doses. Interestingly, the sequence of profiles from Figure 1 is repeated twice. First, for a
219 low number of vaccine doses there is a trade-off between vaccinating the high-mortality individuals
220 in both populations. Then for higher vaccine counts the trade-off is repeated, this time between all
221 individuals of both populations. While this trade-off exists, equitable allocation is heavily favored
222 across almost all levels of available vaccine doses.

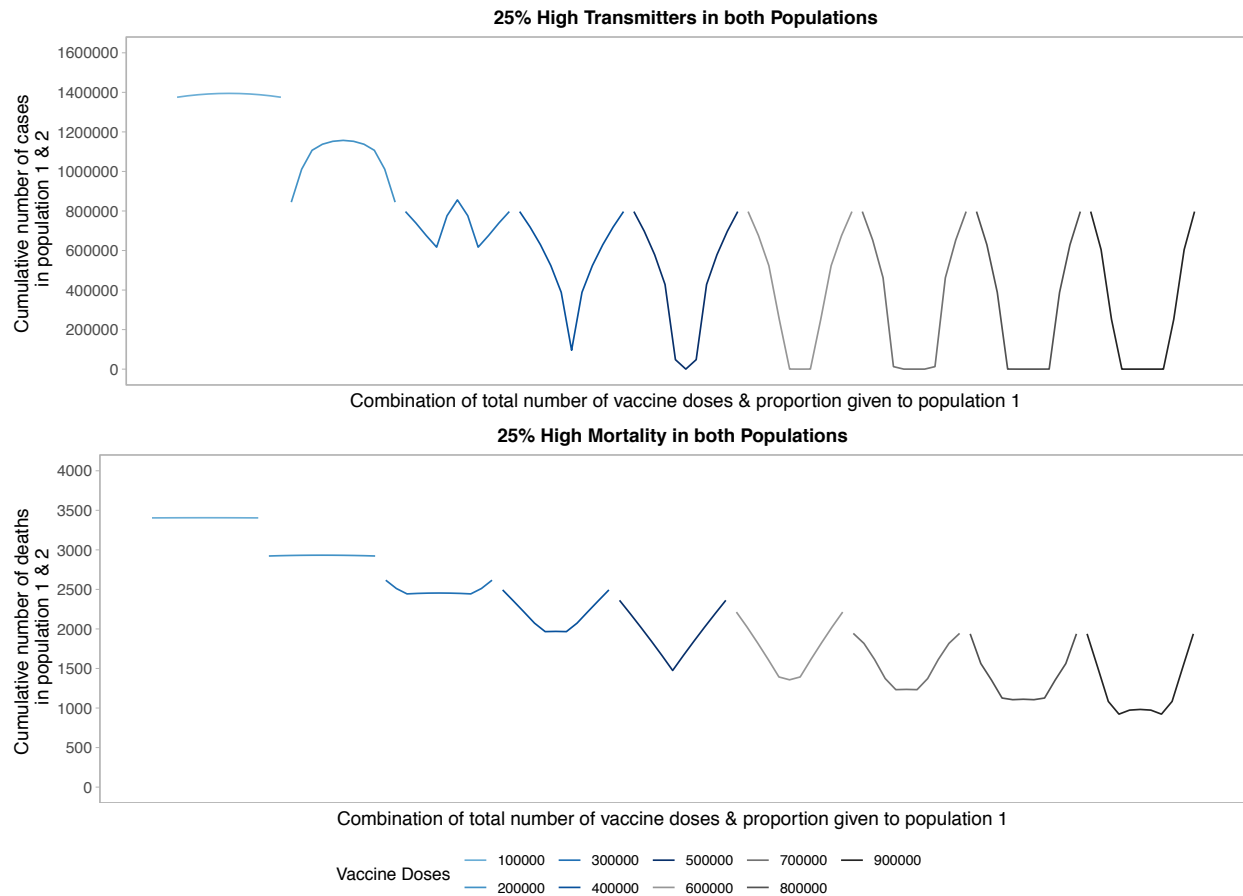


Figure 5: Performance of different allocation strategies of a limited SARS-CoV-2 vaccine stockpile across two heterogeneous populations of equal size (one million individuals) with no underlying immunity and prophylactic vaccination. In both the high transmission scenario (top) and high mortality scenario (bottom), 25% of both populations are high risk.

223 Next we considered the impact of continuous roll-out for both the high transmission and high
 224 mortality scenarios. We find that across both high-risk scenarios and all vaccine roll-out times and
 225 speeds, unequal allocation is highly sub-optimal (Figure 6). Similarly to Figure 4, we vary both
 226 the start date of vaccination roll-out (1, 10, 30, 50, or 100 days) and the daily vaccination rate
 227 (1, 2 or 3% per day). We find that both the speed and timing of vaccine roll-out are important
 228 factors in minimizing the cumulative number of cases or deaths across the two populations, and
 229 see the greatest reduction in cumulative deaths and final size with the earliest and fastest roll-out.
 230 Specifically, for vaccine stockpiles larger than 500,000 doses, the achievable impact of vaccination
 231 is more dependent on the timing (solid vs. dashed curves) and speed (different panels) of vaccine
 232 roll-out rather than on the total number of doses available.

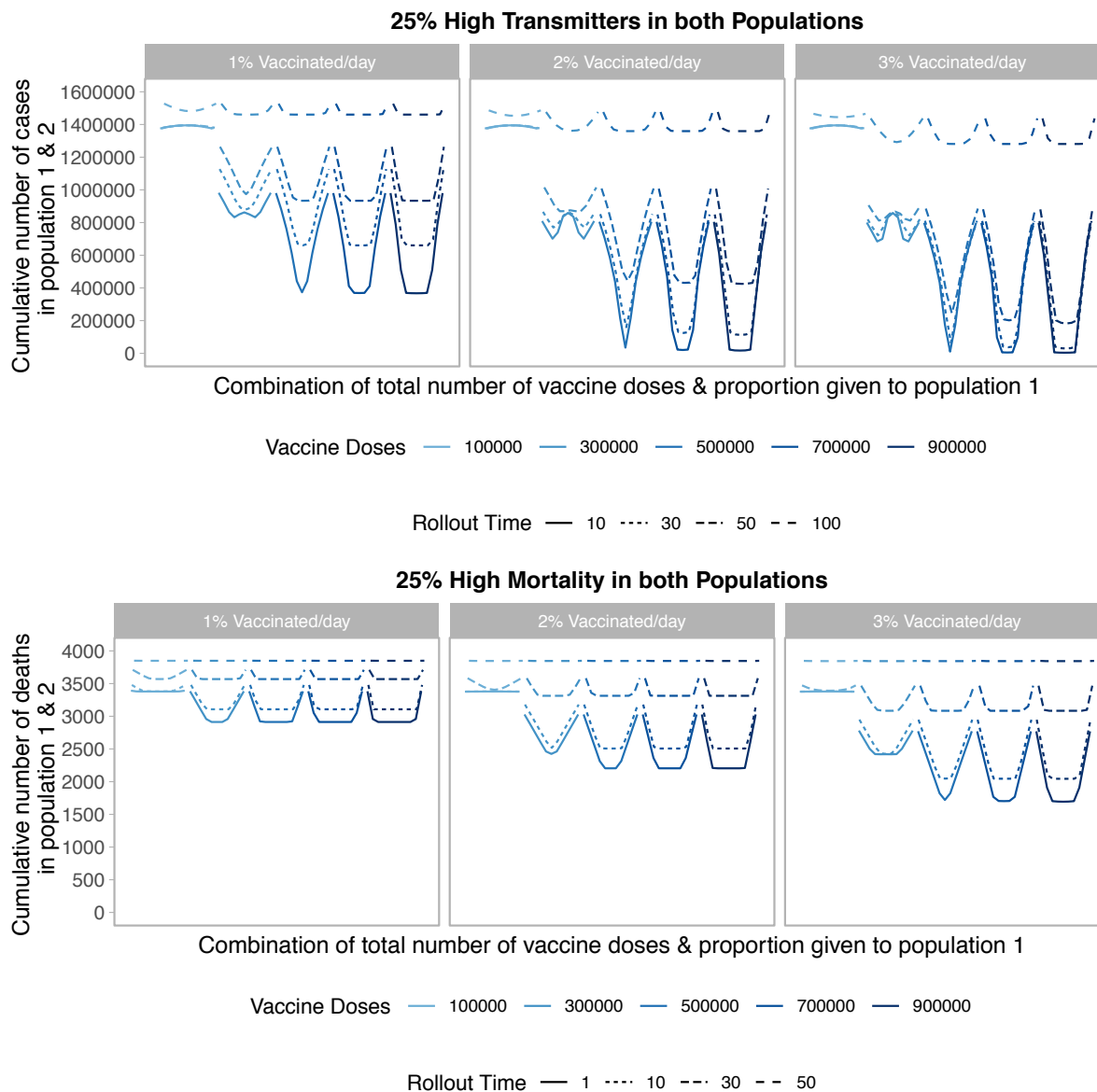


Figure 6: Performance of different allocation strategies of a limited SARS-CoV-2 vaccine stockpile across two heterogeneous populations of equal size (one million individuals) with no underlying immunity, with vaccines rolled out at different speeds and different times after the start of the epidemic. In both the high transmission scenario (top) and high mortality scenario (bottom), 25% of both populations are high risk. We vary the timing of roll-out between 10, 30, 50, or 100 days for the high transmission scenario and 1, 10, 30 or 50 days for the high mortality scenario after the start of the epidemic, and vary the speed of roll-out between 1, 2, or 3% of the population vaccinated per day.

233 5.7 Sensitivity Analyses

234 We assessed the robustness of our results by varying the characteristics of the vaccine and con-
 235 nection between populations to be more representative of the current pandemic. As expected, the
 236 leaky and all-or-nothing vaccine perform identically because both have the same critical vaccination

237 threshold [30] (Figure S1).

238

239 In the previous situations we have only considered the scenario of non-interacting populations.
240 As we relax this strict assumption, we find that as the amount of interaction between the two pop-
241 ulations increases, equitable strategies are most favorable (Figure S2). When the force of infection
242 in each population depends on epidemic dynamics in both populations, accounting for interaction
243 drastically changes the optimal allocation profiles and favors equal allocation between populations,
244 as seen in previous work [11, 15]. Even for low values of the interaction parameter i , equal al-
245 location rapidly becomes optimal. Indeed, for i values higher than 0.01 — which corresponds to
246 one out of every hundred infected individuals contributing to infection in the other population —
247 equal allocation between the two population always performs best. As i further increases, unequal
248 strategies progressively approach the optimal (equal) allocation as indicated by the flattening of the
249 curves. For i equal to 0.5, when the two populations concretely behave like one large population,
250 all allocation strategies perform almost identically. Compared to the non-interacting case, allowing
251 for interaction between the two populations leads to a higher cumulative number of infections for
252 all possible vaccine allocation strategies, and the “W”-shaped allocation curve no longer appears.

253 6 Discussion

254 As countries continue to roll-out vaccines, challenging allocation decisions will need to be made due
255 to resource constraints. Previous studies [11] have shown simple scenarios favor unequal alloca-
256 tion. We recreated those findings, and further apply the theory to the current COVID-19 pandemic.

257

258 In the simple case of two non-interacting populations of identical size we show that for very high
259 quantities of vaccine, relative to population size, equal allocation strategies are optimal. For very
260 few doses, all strategies provide comparable results. This supports the European Commission’s
261 decision to allocate vaccine doses proportional to population size among the 27 European Nations
262 [31]. In this simplest model, until there is enough vaccine for both populations to approach their
263 critical herd immunity threshold, optimal strategies favor a highly unequal approach, allocating
264 doses to either population 1 or 2 until the population has reached its threshold. If the populations
265 vary in size, allocation decisions vary, and as the number of vaccines increases, focus switches from
266 the smaller population to the larger one, as supported by Keeling and Shattock (2012) [11].

267

268 We consider more realistic scenarios that better mirror the current COVID-19 pandemic including
269 underlying immunity, population interaction, continuous vaccine roll-out, and heterogeneous pop-
270 ulation structure. While many of these parameters are either unknown or changing throughout
271 the course of the epidemic, we find that, across a range of scenarios, optimal allocation decisions
272 favor equal allocation across populations. Since these strategies are often optimal or nearly-optimal
273 across a range of parameters, while unequal allocations are only generally optimal for narrow pa-
274 rameter ranges, more equitable strategies might be the best option under uncertainty in an ongoing
275 epidemic.

276

277 Specifically, for scenarios considering heterogeneous population risk, we find that first targeting
278 high risk individuals, either high-transmitters or those at higher risk of death after infection, re-
279 sults in more equal allocations between populations being optimal. Targeting high-risk individuals
280 first, then shifting priority to lower-risk individuals is supported by previous modeling work, looking
281 at SARS-CoV-2 vaccine allocations within a single population [9, 8, 32, 33, 10], and is in concor-

282 dance with the ongoing COVAX strategy, targeting early doses to high-risk individuals, and the
283 USA’s plan to vaccinate health care workers and elderly individuals first [34, 35].

284

285 Our modeling analyses are subject to many simplifying assumptions on population dynamics and
286 vaccine characteristics that may not be applicable to the current pandemic. We consider a vaccine
287 that prevents both SARS-CoV-2 disease and infection, thus providing indirect protection to a frac-
288 tion of the population. Vaccines appear to be able to reduce infectiousness but this effect still needs
289 to be precisely assessed. We do not model vaccine refusal, and assume that all individuals given
290 doses accept them. Recent studies [36] show vaccine hesitancy as a threat to successful COVID-19
291 response. Next, we do not consider delays between doses, but model the epidemic from a final
292 dose which confers 90% efficacy. Due to vaccine shortages, the delay between the first and second
293 dose could impact our findings as individuals may be able to get infected in the interim. Further,
294 we only model one available vaccine. The current SARS-CoV-2 vaccine landscape is complex, and
295 multiple vaccine candidates are rapidly undergoing testing. Considerations for optimal allocation
296 in this context are more complicated, especially if the vaccines have different immunogenicity pro-
297 files, and the quantity of doses and timing of roll-out varies across candidates. Further, we only
298 consider one strain of SARS-CoV-2, not taking into account variants with varying transmissibility
299 and mortality. Finally, we do not consider the impact of non-pharmaceutical interventions (NPIs)
300 in conjunction with vaccination.

301

302 Furthermore, we only model allocation strategies within two symmetric populations. It is likely
303 that policy makers will face allocation decisions across multiple countries, or across multiple regions
304 within a country. While our analyses do not extend to more than two locations, general principles
305 should remain the same, as illustrated for three populations in Duijzer et al. (2018) [15] and Keeling
306 and Shattock (2012) [11].

307

308 Future modeling work on SARS-CoV-2 vaccination strategies is needed, as multiple vaccine can-
309 didates continue to be rolled out. These studies should also consider the effects of vaccines on
310 reducing hospitalizations and preserving hospital capacity, which may have indirect benefits for
311 mortality rates for COVID-19 and other diseases beyond the direct prevention of infection in high-
312 risk populations. In addition, other work should also consider populations with varying epidemic
313 dynamics, and distribution capacity. Indeed, it has been argued that populations at higher imme-
314 diate risk of SARS-CoV-2 spread and populations where vaccine roll-out is most efficient should be
315 prioritized for SARS-CoV-2 vaccine allocation [37].

316

317 With vaccine supplies still severely constrained, rapid allocation decisions will need to be made.
318 Due to the magnitude of SARS-CoV-2 spread and impact globally, further political and economic
319 constraints will likely play a large role in allocation decisions. Mathematical modelling can provide
320 insight into optimal allocation strategies that maximize the benefit from each dose. Conclusions
321 from such models should be balanced with ethical considerations on the fairness of allocation that
322 also minimize disparities in access. We show key principles that should be considered in the design
323 of realistic and implementable allocation strategies.

324 7 Acknowledgments

325 We thank Dr. Kendall Hoyt for helpful discussion. ER, LKS and ML were supported by the
326 Morris-Singer Fund. This work was supported in part by Award Number U01CA261277 from the

327 US National Cancer Institute of the National Institutes of Health. The content of this article is
328 solely the responsibility of the authors and does not necessarily represent the official views of the
329 Morris-Singer Fund or the National Institutes of Health.

References

- 330
- 331 [1] Ensheng Dong, Hongru Du, and Lauren Gardner. An interactive web-based dashboard to
332 track COVID-19 in real time. *The Lancet Infectious Diseases*, 20(5):533–534, May 2020.
- 333 [2] Carl Zimmer, Jonathan Corum, and Sui-Lee Wee. Coronavirus Vaccine Tracker. *The New*
334 *York Times*.
- 335 [3] Madhumita Shrotri, Tui Swinnen, Beate Kampmann, and Edward P K Parker. An interactive
336 website tracking COVID-19 vaccine development. *The Lancet Global Health*, 9(5):e590–e592,
337 May 2021.
- 338 [4] Edouard Mathieu, Hannah Ritchie, Esteban Ortiz-Ospina, Max Roser, Joe Hasell, Cameron
339 Appel, Charlie Giattino, and Lucas Rodés-Guirao. A global database of COVID-19 vaccina-
340 tions. *Nature Human Behaviour*, May 2021.
- 341 [5] CEPI, Gavi, and WHO. COVAX Global Supply Forecast, January 2021.
- 342 [6] Aisling Irwin. What it will take to vaccinate the world against COVID-19. *Nature*,
343 592(7853):176–178, March 2021. Number: 7853 Publisher: Nature Publishing Group.
- 344 [7] Wellcome. When will the world be vaccinated against Covid-19?, January 2021.
- 345 [8] Kate M Bubar, Stephen M Kissler, Marc Lipsitch, Sarah Cobey, Yonatan Grad, and Daniel B
346 Larremore. Model-informed COVID-19 vaccine prioritization strategies by age and serostatus.
347 preprint, *Infectious Diseases (except HIV/AIDS)*, September 2020.
- 348 [9] Laura Matrajt, Julia Eaton, Tiffany Leung, and Elizabeth R. Brown. Vaccine optimization
349 for COVID-19: who to vaccinate first? preprint, *Epidemiology*, August 2020.
- 350 [10] A Hogan, P Winskill, O Watson, P Walker, C Whittaker, M Baguelin, D Haw, A Lochen,
351 K Gaythorpe, K Ainslie, S Bhatt, A Boonyasiri, O Boyd, N Brazeau, L Cattarino, G Charles,
352 L Cooper, H Coupland, Z Cucunuba Perez, G Cuomo-Dannenburg, C Donnelly, I Dorigatti,
353 O Eales, S Van Elsland, F Ferreira Do Nascimento, R Fitzjohn, S Flaxman, W Green, T Hallett,
354 A Hamlet, W Hinsley, N Imai, E Jauneikaite, B Jeffrey, E Knock, D Laydon, J Lees, T Mellan,
355 S Mishra, G Nedjati Gilani, P Nouvellet, A Ower, K Parag, M Ragonnet-Cronin, I Siveroni,
356 J Skarp, H Thompson, H Unwin, R Verity, M Vollmer, E Volz, C Walters, H Wang, Y Wang,
357 L Whittles, X Xi, F Muhib, P Smith, K Hauck, N Ferguson, and A Ghani. Report 33:
358 Modelling the allocation and impact of a COVID-19 vaccine. Technical report, Imperial College
359 London, September 2020.
- 360 [11] Matt J. Keeling and Andrew Shattock. Optimal but unequitable prophylactic distribution of
361 vaccine. *Epidemics*, 4(2):78–85, June 2012.
- 362 [12] Edward Goldstein, Marc Lipsitch, and Muge Cevik. On the effect of age on the transmission
363 of SARS-CoV-2 in households, schools and the community. preprint, *Epidemiology*, July 2020.
- 364 [13] Fei Zhou, Ting Yu, Ronghui Du, Guohui Fan, Ying Liu, Zhibo Liu, Jie Xiang, Yeming Wang,
365 Bin Song, Xiaoying Gu, Lulu Guan, Yuan Wei, Hui Li, Xudong Wu, Jiuyang Xu, Shengjin
366 Tu, Yi Zhang, Hua Chen, and Bin Cao. Clinical course and risk factors for mortality of
367 adult inpatients with COVID-19 in Wuhan, China: a retrospective cohort study. *The Lancet*,
368 395(10229):1054–1062, March 2020.

- 369 [14] Chaomin Wu, Xiaoyan Chen, Yanping Cai, Jia'an Xia, Xing Zhou, Sha Xu, Hanping Huang,
370 Li Zhang, Xia Zhou, Chunling Du, Yuye Zhang, Juan Song, Sijiao Wang, Yencheng Chao,
371 Zeyong Yang, Jie Xu, Xin Zhou, Dechang Chen, Weining Xiong, Lei Xu, Feng Zhou, Jin-
372 jun Jiang, Chunxue Bai, Junhua Zheng, and Yuanlin Song. Risk Factors Associated With
373 Acute Respiratory Distress Syndrome and Death in Patients With Coronavirus Disease 2019
374 Pneumonia in Wuhan, China. *JAMA Internal Medicine*, 180(7):934, July 2020.
- 375 [15] Lotty E. Duijzer, Willem L. van Jaarsveld, Jacco Wallinga, and Rommert Dekker. Dose-
376 Optimal Vaccine Allocation over Multiple Populations. *Production and Operations Manage-*
377 *ment*, 27(1):143–159, January 2018.
- 378 [16] Joseph T Wu, Steven Riley, and Gabriel M Leung. Spatial considerations for the allocation of
379 pre-pandemic influenza vaccination in the United States. *Proceedings of the Royal Society B:*
380 *Biological Sciences*, 274(1627):2811–2817, November 2007.
- 381 [17] P. Klepac, R. Laxminarayan, and B. T. Grenfell. Synthesizing epidemiological and economic
382 optima for control of immunizing infections. *Proceedings of the National Academy of Sciences*,
383 108(34):14366–14370, August 2011.
- 384 [18] G. A. Forster and C. A. Gilligan. Optimizing the control of disease infestations at the landscape
385 scale. *Proceedings of the National Academy of Sciences*, 104(12):4984–4989, March 2007.
- 386 [19] Robert E. Rowthorn, Ramanan Laxminarayan, and Christopher A. Gilligan. Optimal control
387 of epidemics in metapopulations. *Journal of The Royal Society Interface*, 6(41):1135–1144,
388 December 2009.
- 389 [20] Laura Matrajt and Ira M. Longini. Optimizing Vaccine Allocation at Different Points in Time
390 during an Epidemic. *PLoS ONE*, 5(11):e13767, November 2010.
- 391 [21] Sido D. Mylius, Thomas J. Hagenaars, Anna K. Lugnér, and Jacco Wallinga. Optimal alloca-
392 tion of pandemic influenza vaccine depends on age, risk and timing. *Vaccine*, 26(29-30):3742–
393 3749, July 2008.
- 394 [22] Anna Teytelman and Richard C. Larson. Multiregional Dynamic Vaccine Allocation During
395 an Influenza Epidemic. *Service Science*, 5(3):197–215, September 2013.
- 396 [23] Edwin C. Yuan, David L. Alderson, Sean Stromberg, and Jean M. Carlson. Optimal Vac-
397 cination in a Stochastic Epidemic Model of Two Non-Interacting Populations. *PLOS ONE*,
398 10(2):e0115826, February 2015.
- 399 [24] Chantal Nguyen and Jean M. Carlson. Optimizing Real-Time Vaccine Allocation in a Stochas-
400 tic SIR Model. *PLOS ONE*, 11(4):e0152950, April 2016.
- 401 [25] Eli S. Rosenberg, James M. Tesoriero, Elizabeth M. Rosenthal, Rakkoo Chung, Meredith A.
402 Barranco, Linda M. Styer, Monica M. Parker, Shu-Yin John Leung, Johanne E. Morne,
403 Danielle Greene, David R. Holtgrave, Dina Hoefler, Jessica Kumar, Tomoko Udo, Brad Hutton,
404 and Howard A. Zucker. Cumulative incidence and diagnosis of SARS-CoV-2 infection in New
405 York. *Annals of Epidemiology*, 48:23–29.e4, August 2020.
- 406 [26] Public Health England. Sero-surveillance of COVID-19. Technical report, October 2020.

- 407 [27] Marina Pollán, Beatriz Pérez-Gómez, Roberto Pastor-Barriuso, Jesús Oteo, Miguel A
408 Hernán, Mayte Pérez-Olmeda, Jose L Sanmartín, Aurora Fernández-García, Israel Cruz,
409 Nerea Fernández de Larrea, Marta Molina, Francisco Rodríguez-Cabrera, Mariano Martín,
410 Paloma Merino-Amador, Jose León Paniagua, Juan F Muñoz-Montalvo, Faustino Blanco,
411 Raquel Yotti, Faustino Blanco, Rodrigo Gutiérrez Fernández, Mariano Martín, Saturnino
412 Mezcua Navarro, Marta Molina, Juan F. Muñoz-Montalvo, Matías Salinero Hernández,
413 Jose L. Sanmartín, Manuel Cuenca-Estrella, Raquel Yotti, José León Paniagua, Nerea
414 Fernández de Larrea, Pablo Fernández-Navarro, Roberto Pastor-Barriuso, Beatriz Pérez-
415 Gómez, Marina Pollán, Ana Avellón, Giovanni Fedele, Aurora Fernández-García, Jesús
416 Oteo Iglesias, María Teresa Pérez Olmeda, Israel Cruz, Maria Elena Fernandez Martinez,
417 Francisco D. Rodríguez-Cabrera, Miguel A. Hernán, Susana Padrones Fernández, José Manuel
418 Rumbao Aguirre, José M. Navarro Marí, Begoña Palop Borrás, Ana Belén Pérez Jiménez,
419 Manuel Rodríguez-Iglesias, Ana María Calvo Gascón, María Luz Lou Alcaine, Ignacio Do-
420 nate Suárez, Oscar Suárez Álvarez, Mercedes Rodríguez Pérez, Margarita Cases Sanchís,
421 Carlos Javier Villafáfila Gomila, Lluís Carbo Saladrigas, Adoración Hurtado Fernández,
422 Antonio Oliver, Elías Castro Feliciano, María Noemí González Quintana, José María Bar-
423 rassa Fernández, María Araceli Hernández Betancor, Melisa Hernández Febles, Leopoldo
424 Martín Martín, Luis-Mariano López López, Teresa Ugarte Miota, Inés De Benito Población,
425 María Sagrario Celada Pérez, María Natalia Vallés Fernández, Tomás Maté Enríquez, Miguel
426 Villa Arranz, Marta Domínguez-Gil González, Isabel Fernández-Natal, Gregoria Megías Lobón,
427 Juan Luis Muñoz Bellido, Pilar Ciruela, Ariadna Mas i Casals, Maria Doladé Botías, M. Ange-
428 les Marcos Maeso, Dúnia Pérez del Campo, Antonio Félix de Castro, Ramón Limón Ramírez,
429 Maria Francisca Elías Retamosa, Manuela Rubio González, María Sinda Blanco Lobeiras,
430 Alberto Fuentes Losada, Antonio Aguilera, German Bou, Yolanda Caro, Noemí Marauri,
431 Luis Miguel Soria Blanco, Isabel del Cura González, Montserrat Hernández Pascual, Roberto
432 Alonso Fernández, Paloma Merino-Amador, Natalia Cabrera Castro, Aurora Tomás Lizcano,
433 Cristóbal Ramírez Almagro, Manuel Segovia Hernández, Nieves Ascunce Elizaga, María Ed-
434 erra Sanz, Carmen Ezpeleta Baquedano, Ana Bustinduy Bascaran, Susana Iglesias Tamayo,
435 Luis Elorduy Otazua, Rebeca Benarroch Benarroch, Jesús Lopera Flores, and Antonia Vázquez
436 de la Villa. Prevalence of SARS-CoV-2 in Spain (ENE-COVID): a nationwide, population-
437 based seroepidemiological study. *The Lancet*, 396(10250):535–544, August 2020.
- 438 [28] Henrik Salje, Cécile Tran Kiem, Noémie Lefrancq, Noémie Courtejoie, Paolo Bosetti, Juli-
439 ette Paireau, Alessio Andronico, Nathanaël Hozé, Jehanne Richet, Claire-Lise Dubost, Yann
440 Le Strat, Justin Lessler, Daniel Levy-Bruhl, Arnaud Fontanet, Lulla Opatowski, Pierre-Yves
441 Boelle, and Simon Cauchemez. Estimating the burden of SARS-CoV-2 in France. *Science*,
442 369(6500):208–211, July 2020.
- 443 [29] Shamez N Ladhani, Anna Jeffery-Smith, Monika Patel, Roshni Janarthanan, Jonathan Fok,
444 Emma Crawley-Boevey, Amoolya Vusirikala, Elena Fernandez Ruiz De Olano, Marina Sanchez
445 Perez, Suzanne Tang, Kate Dun-Campbell, Edward Wynne Evans, Anita Bell, Bharat Patel,
446 Zahin Amin-Chowdhury, Felicity Aiano, Karthik Paranthaman, Thomas Ma, Maria Saavedra-
447 Campos, Joanna Ellis, Meera Chand, Kevin Brown, Mary E. Ramsay, Susan Hopkins, Nandini
448 Shetty, J. Yimmy Chow, Robin Gopal, and Maria Zambon. High prevalence of SARS-CoV-2
449 antibodies in care homes affected by COVID-19: Prospective cohort study, England. *EClini-
450 calMedicine*, 28:100597, November 2020.
- 451 [30] F. M. G. Magpantay, M. A. Riolo, M. Domenech de Cellès, A. A. King, and P. Rohani.
452 Epidemiological Consequences of Imperfect Vaccines for Immunizing Infections. *SIAM Journal*

- 453 *on Applied Mathematics*, 74(6):1810–1830, January 2014.
- 454 [31] European Commission. Communication from the Commission EU Strategy for COVID-19
455 vaccines, June 2020.
- 456 [32] Sam Moore, Edward M Hill, Louise Dyson, Michael Tildesley, and Matt J Keeling. Modelling
457 optimal vaccination strategy for SARS-CoV-2 in the UK. preprint, *Epidemiology*, September
458 2020.
- 459 [33] Xin Chen, Menglong Li, David Simchi-Levi, and Tiancheng Zhao. Allocation of COVID-19
460 Vaccines Under Limited Supply. preprint, *Infectious Diseases (except HIV/AIDS)*, August
461 2020.
- 462 [34] World Health Organization. *WHO Concept for fair access and equitable allocation of COVID-
463 19 health products*. September 2020.
- 464 [35] Committee on Equitable Allocation of Vaccine for the Novel Coronavirus, Board on Health
465 Sciences Policy, Board on Population Health and Public Health Practice, Health and Medicine
466 Division, and National Academies of Sciences, Engineering, and Medicine. *Framework for
467 Equitable Allocation of COVID-19 Vaccine*. National Academies Press, Washington, D.C.,
468 2020. Pages: 25917.
- 469 [36] Amiel A. Dror, Netanel Eisenbach, Shahar Taiber, Nicole G. Morozov, Matti Mizrachi, Asaf
470 Zigran, Samer Srouji, and Eyal Sela. Vaccine hesitancy: the next challenge in the fight against
471 COVID-19. *European Journal of Epidemiology*, 35(8):775–779, August 2020.
- 472 [37] Ezekiel J. Emanuel and Govind Persad. This Is the Wrong Way to Distribute Badly Needed
473 Vaccines, May 2021.
- 474 [38] Evelot Duijzer, Willem van Jaarsveld, Jacco Wallinga, and Rommert Dekker. The most effi-
475 cient critical vaccination coverage and its equivalence with maximizing the herd effect. *Math-
476 ematical Biosciences*, 282:68–81, December 2016.